Novel Modification of Shock-Tube Facility for Strain-Testing of Carbon Fiber Airframes Under Impulsive Shock Loading

Jonathan W. Zak[1]
Vanderbilt University, Nashville, TN, 37235, USA

Amrutur V. Anilkumar[2]
Vanderbilt University, Nashville, TN, 37235, USA

A novel shock-tube-based experimental facility has been developed to investigate the dynamic strain response of cylindrical carbon fiber composite structures under controlled impulsive internal pressure loading and end wall reflection. The facility integrates cylindrical test sections into a conventional shock tube, transforming the apparatus into a structural testing platform where composite and metallic specimens are subjected to loading from incident and reflected shock waves. A Carbon fiber test section with [0/90/0] symmetric layup and an aluminum 6061-T6 reference specimen were instrumented with resistive strain gauges (RSG) and Fiber Bragg Grating (FBG) sensors to capture time-resolved axial and hoop strain histories during shock loading and end wall reflection. Experimental results reveal differences in strain coupling behavior between materials. Aluminum specimens exhibited strong Poisson coupling with synchronized 2:1 hoop-to-axial strain ratio and synchronized frequency content throughout the loading event. In contrast, the carbon fiber composite showed weak coupling, arising from the orthotropic layup architecture. This novel facility provides a controlled platform for investigating dynamic material response, pre-strain effects, and structural-health-monitoring sensor validation under impulsive loading conditions.

I. Introduction

Composite airframe structures in reusable launch vehicles experience transient internal pressure loads during routine operations, including stage separation events and rapid depressurization. Accurately characterizing the dynamic strain response of carbon fiber reinforced polymer (CFRP) cylinders under such loading is essential for flight-based structural health monitoring and re-flight certification. The study of carbon fiber cylinders under gas dynamic loading remains limited [1-3]. This study outlines an experimental facility for studying the high strain-rate response of composite structures under controlled shock loading.

Carbon fiber composites exhibit orthotropic material behavior that depends strongly on fiber orientation and laminate layup [4-5]. When subjected to internal pressure, composite cylinders experience coupled hoop and axial strain that differs fundamentally from the isotropic response of metallic structures. Analytical prediction of these coupling effects is challenging, particularly for short-duration pressure transients with rise times on the order of milliseconds.

Existing experimental approaches for characterizing composite cylinder dynamic response typically rely on quasi-static pressure testing or impact surrogates [6-9]. Shock tubes offer a means of applying rapid, repeatable internal pressure transients with well-defined temporal characteristics [10]. Integration of cylindrical test sections into a

[1] Graduate Student, Department of Mechanical Engineering, AIAA Student Member 1741857.
[2] Professor of Practice of Aerospace Engineering, Department of Mechanical Engineering, AIAA Associate Fellow.

conventional shock tube requires careful attention to structural attachment, sealing, and load transfer while maintaining safety under high internal pressure.

Fiber Bragg Grating (FBG) sensors offer distinct advantages over conventional resistive strain gauges (RSGs), including immunity to electromagnetic interference, low sensor mass, and the ability to multiplex multiple sensing locations along a single optical fiber, making them appealing for in-flight integration [11-14].

The objective of the present work is to demonstrate a modified shock-tube-based facility where the axial and hoop strain are studied in cylindrical sections under incident and reflected shock loading. A CFRP cylinder with a controlled fiber layup is tested alongside an isotropic aluminum reference specimen to reveal differences in strain coupling and dynamic response. The facility provides a repeatable platform for investigating dynamic structural response and establishes a foundation for further studies on laminate layup configuration, pre-strain effects, defect identification and structural health monitoring sensor validation.

II. Experimental Approach

The experimental framework was structured to meet three primary objectives. First, the test protocol was required to recreate high dynamic loading conditions while maintaining repeatability and instrumentation survivability. Second, the instrumentation architecture was designed to validate high strain-rate sensing using RSG sensors, with FBG used for cross-comparison. Third, the experiments were intended to characterize the strain response of composite cylinders relative to isotropic reference materials, in the context of shock reflection of the end wall

A. Experimental Facility and Design

The facility modification adds a cylindrical composite or a metallic section to the existing driven section of the shock tube, enabling the added structure to experience transient internal pressure loading as the shock propagates through it and reflects at the end wall. This modification transforms a conventional shock tube into a structural testing platform where the configurable test article is subjected to controlled gas-dynamic loading. Additionally, the driven section is modified such that it can be pressurized or evacuated prior to diaphragm rupture, enabling investigation of pre-strain effects. This capability is particularly relevant for composite structures that may experience both static and dynamic loading during flight operations.

Upon diaphragm rupture, a shock wave propagates through the driven section and pressurizes the interior of the test specimen, producing a rapid circumferential-dominated strain response. When the shock reaches the closed end wall, two critical events occur simultaneously: the shock reflects with higher pressure magnitude, and a one-dimensional axial loading is induced in the cylindrical structure. This interaction is essential for observing circumferential and axial strain coupling, as the wall constraint drives axial structural response and oscillations. The coupling between hoop and axial strain during this reflected phase reveals differences between isotropic and orthotropic material behavior.

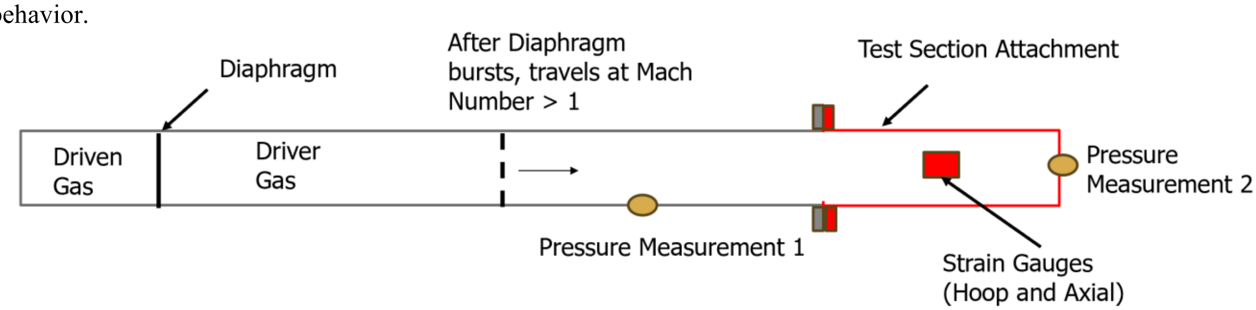

Fig. 1 Schematic of shock tube facility modification showing driver section, diaphragm location, cylindrical test section integration and configuration. Pressure transducer locations and typical shock propagation sequence are indicated.

B. Test Section Design

Integration of a thin-walled composite cylinder into the shock tube driven section required a structural attachment capable of withstanding internal pressure loads while maintaining pressure sealing and alignment. The attachment system must transfer axial loads during shock reflection to the test specimen without introducing stress concentrations or compromising shock wave propagation.

The attachment approach employs a custom-machined steel flange and endcap, bonded to each end of the cylindrical test section using high-shear-strength structural adhesive. The flange and endcap feature a 2-inch bonding length to distribute axial loads uniformly across the composite wall thickness. 3M DP420 two-part epoxy with a rated shear strength of 4500 psi was selected as the adhesive based on compatibility with carbon fiber substrates and resistance to temperature variations during testing.

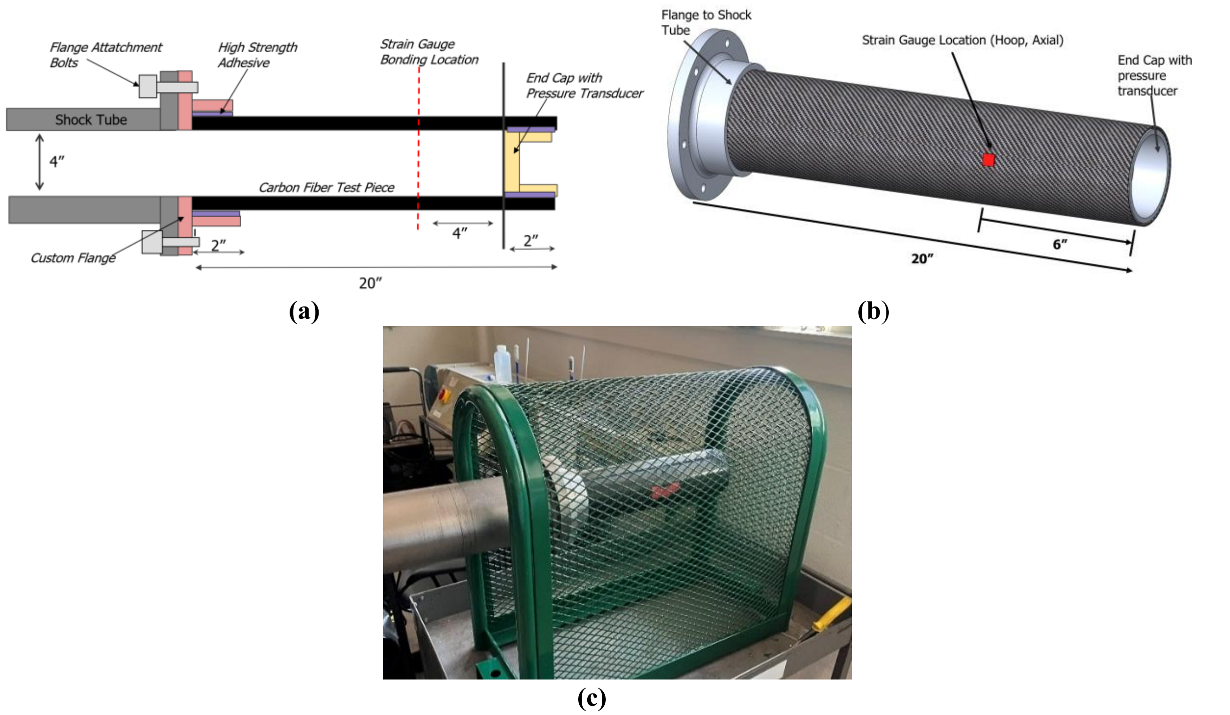

Fig. 2 Cylindrical test section assembly showing (a) cross section schematic with flange attachment; (b) CAD model of carbon fiber test piece; (c) As-built test section mounted on shock tube protected by steel mesh safety cage

C. Instrumentation Architecture

Dynamic strain measurement was accomplished using surface-mounted RSG and FBG strain sensors. Both sensor types were mounted 4 inches from the end wall to capture hoop and axial strain components during shock loading.

FBG strain sensors operate on the principle of wavelength-selective reflection within an optical fiber containing a periodic refractive index variation. Mechanical strain alters the grating period, producing a measurable shift in the reflected Bragg wavelength. For the present experiments, polyimide-coated FBG sensors with Bragg wavelengths ranging from 1546 nm to 1561 nm were used. The wavelength spacing of 6 nm between adjacent sensors provided a strain measurement range of ±5000 micro strain per sensor.

FBG sensors were bonded to the outer surface of the test specimens using M-Bond GA-2 epoxy, consistent with standard FBG adhesion practice. Hoop-oriented sensors were aligned circumferentially, while axial sensors were aligned parallel to the cylinder axis.

Resistive strain gauges (350-ohm linear gauges with gauge factor of 2.12) were bonded and co-located with selected FBG sensors to enable direct performance comparison. The RSGs were configured in quarter-bridge circuits with temperature-compensated completion resistors and signal conditioning amplifiers providing 10 kHz sensing bandwidth. FBG and RSG data were sampled at 35 kHz and 100 kHz respectively, with the data being time synchronized via the pressure transducer trigger.

D. Shock Tube Simulations

Shock propagation simulations using the *University of Wisconsin* shock tube simulator [15] were conducted to optimize sensor placement. The simulations indicated that positioning sensors 4 inches from the end wall would capture the steepest pressure rise in the shortest time following shock reflection, maximizing the observable dynamic strain response. This location was sufficiently distant from the end wall attachment to avoid end effects from the bonded joint while remaining close enough to the end wall to capture the reflected shock interaction that drives axial loading and strain coupling.

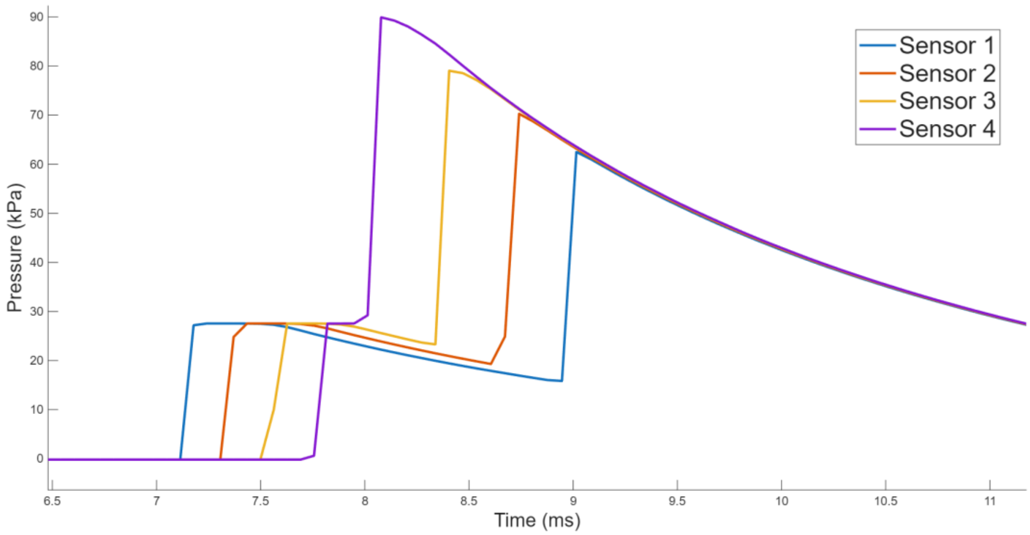

(a)

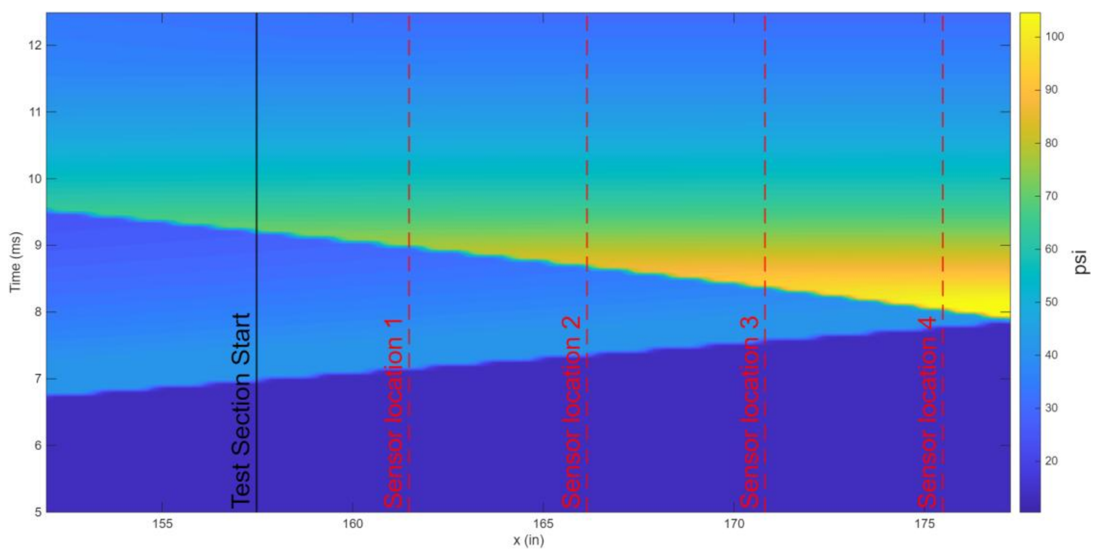

(b)

Fig. 3 (a)Simulated pressure-time history at different test section locations for a Mach 1.36 shock, showing incident shock arrival, pressure plateau, reflected shock arrival, and weakening. (b)X-t diagram shows shock propagation and reflection sequence in test section.

III. Results

The experimental study was conducted in three phases to systematically characterize facility performance and material response. Initial tests established baseline facility performance through calibration and repeatability assessment. Subsequent dynamic tests compared aluminum and carbon fiber composite specimens under identical shock loading conditions. Finally, FBG sensor performance was validated against conventional strain gauges, and the test facility's pre-strain capability was demonstrated.

A. Isotropic Response: Aluminum 6061

The aluminum specimen provided a well-characterized isotropic baseline for comparison with composite specimen strain response and strain coupling behavior.

Figure 4 presents simultaneous hoop and axial strain measurements for an aluminum specimen subjected to shock loading. The strain response exhibits a characteristic two-stage profile corresponding to incident and reflected shock loading.

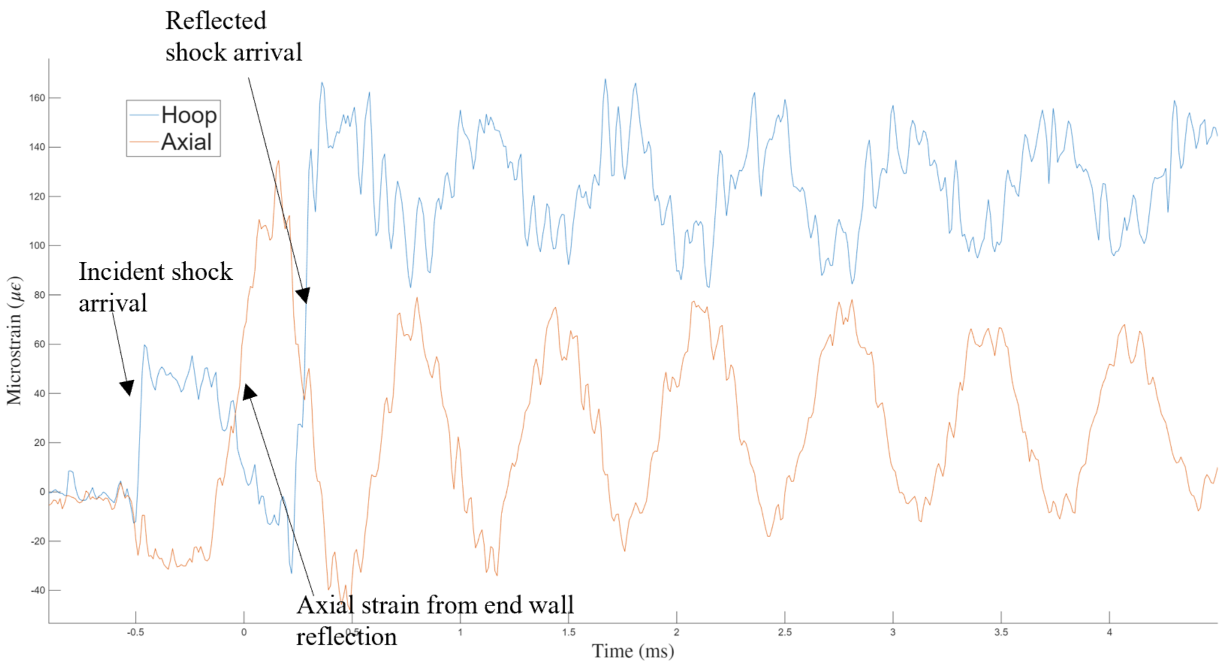

Fig 4. Aluminum hoop and axial strain time histories during shock loading and end wall reflection.

Upon reflected shock, hoop strain peaks to approximately 150 micro strain while axial strain reaches approximately 75 micro strain.

Following peak loading, both hoop and axial strains exhibit synchronized oscillatory behavior at the same frequency. This temporal correlation confirms that the aluminum structure responds as an isotropic system, where deformation in one direction necessarily induces proportional strain in the orthogonal direction through the material's Poisson ratio.

Fast Fourier Transform (FFT) analysis of the aluminum strain signals demonstrates the strong coupling between hoop and axial directions, characteristic of isotropic material behavior.

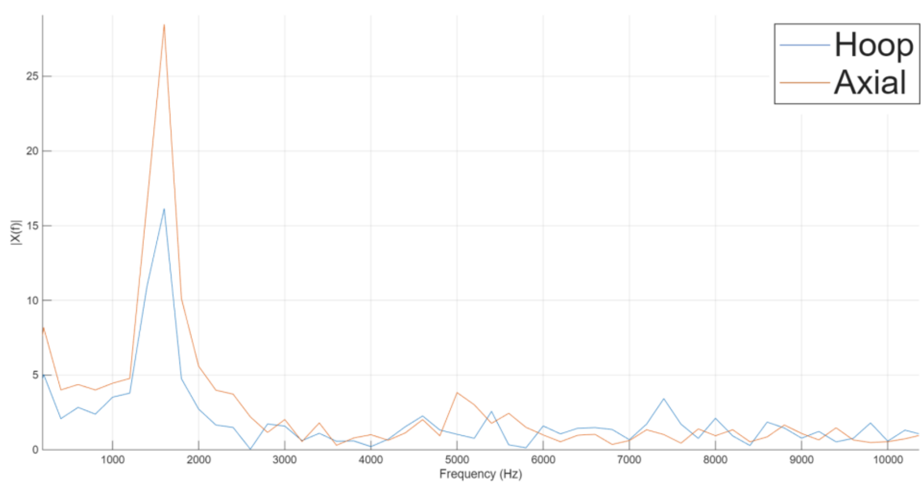

Fig. 5 FFT analysis of aluminum specimen overlaying hoop and axial strain frequency spectra.

Both hoop and axial strain spectra exhibit dominant frequency content at the same characteristic frequencies. This shared frequency content confirms strong Poisson coupling, where structural motion in one direction necessarily excites corresponding motion in the orthogonal direction. The synchronized frequency response is consistent with isotropic material behavior, where the elastic properties are identical in all directions.

B. Orthotropic Composite Response: Carbon Fiber

The carbon fiber composite specimen exhibited distinctly different strain response characteristics compared to aluminum, revealing the influence of material orthotropy and fiber orientation on dynamic structural behavior. Under identical shock loading conditions, the CFRP specimen exhibited weak coupling between hoop and axial directions compared to aluminum.

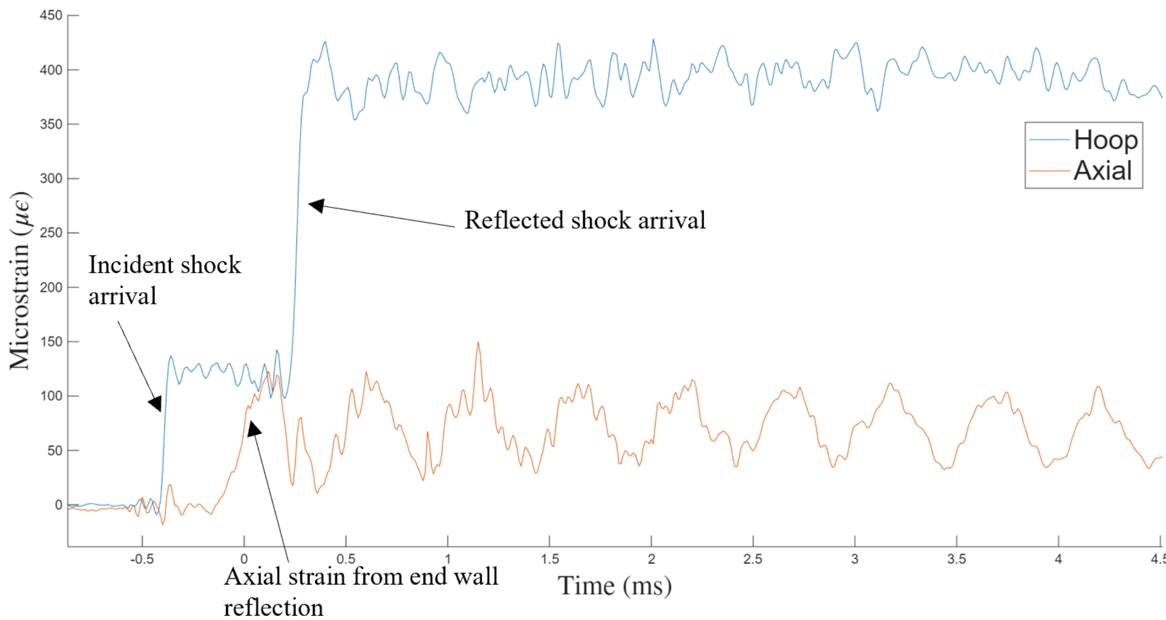

Fig. 6 Carbon Fiber specimen hoop and axial strain time histories during shock loading and end wall reflection.

The CFRP hoop strain reached a peak of approximately 400-450 micro strain, significantly higher than the 150 micro strain observed in aluminum under identical loading conditions. This higher circumferential strain reflects the lower circumferential stiffness due to the chosen fiber layup composition [0/0/90]. The CFRP axial strain exhibited minimal response during the primary hoop loading phase of shock transmission and showed oscillatory behavior that was non-dependent on the axial strain oscillations induced by the axial loading of the shock hitting the end wall.

In the aluminum specimen, hoop and axial strains exhibited clear temporal correlation, with oscillations occurring in phase and maintaining an approximate 2:1 magnitude ratio throughout the loading event. In contrast, the CFRP specimen showed minimal axial strain during hoop loading, whereas the axial response dominated by oscillations did not couple strongly to hoop response. This weak coupling is attributable to the layup-dependent effective Poisson's ratios in composite laminates and the non-homogenous nature of the carbon fiber layer stacking and possibly dissipation in the interfacial layers.

FFT analysis revealed that the orthotropic CFRP specimen exhibits fundamentally different frequency characteristics compared to aluminum, with independent modal behavior in the hoop and axial directions.

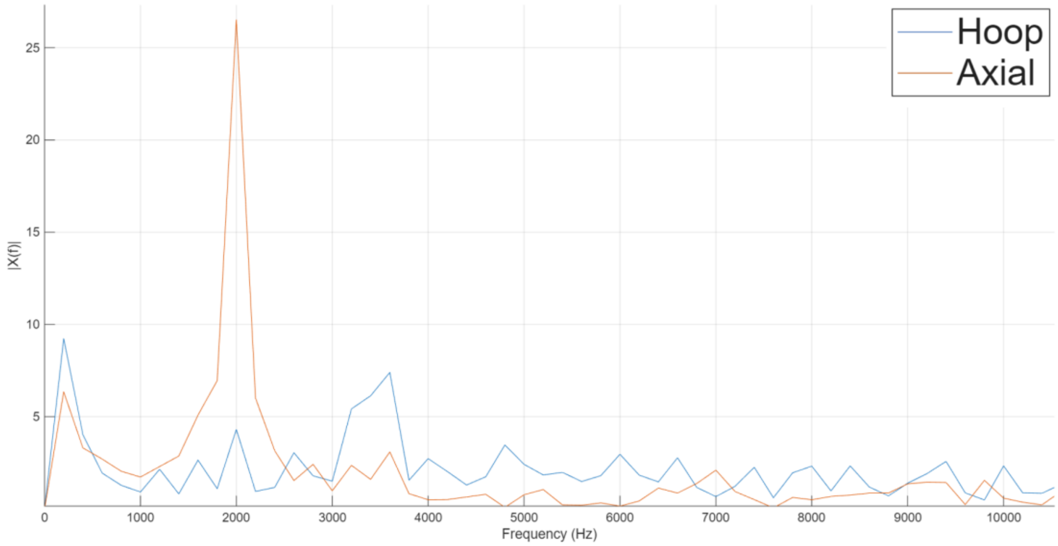

Fig. 7 FFT analysis of carbon fiber specimen showing hoop and axial strain frequency spectra overlaid.

C. FBG vs RSG Performance Comparison

Under shock tube loading conditions, FBG and RSG sensors showed good temporal correlation and comparable strain magnitudes.

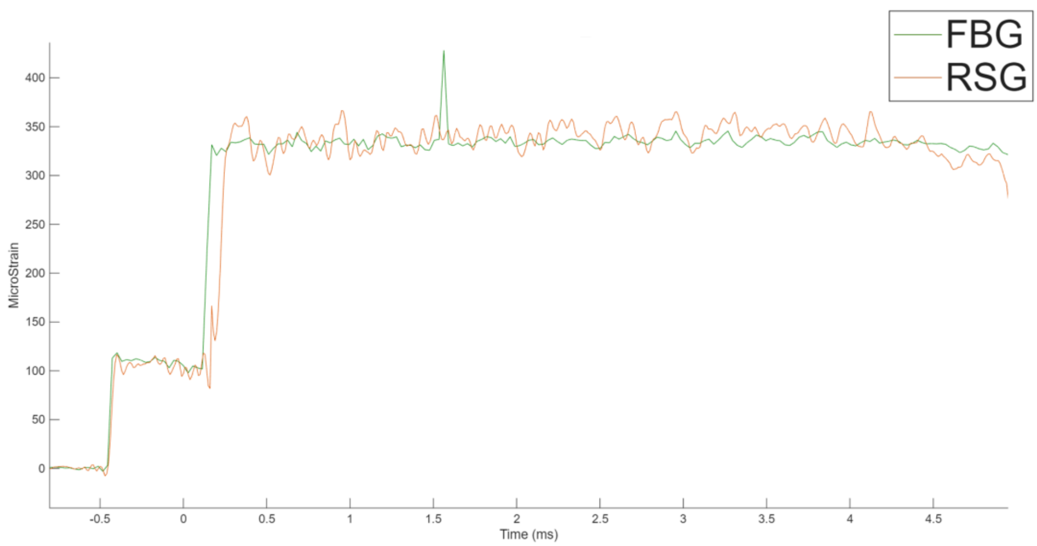

Fig. 8 Co-located FBG and RSG hoop strain measurements during shock tube testing

For the carbon fiber specimen at 105 psi burst pressure, co-located FBG and RSG sensors measured hoop strains at a 4% difference in detected mean strain values, best explained by the different geometries of FBG and RSG sensors. RSG are bonded as a grid of 0.25” by 0.125” forming an area measurement, while FBG are bonded as a linear sensor of length 0.3”. Additionally, RSG strain is found from converting a change in resistance to a voltage proportional to the strain while the optically determined strain in the FBG is determined from peak-tracking algorithms of the wavelength data. The temporal evolution of both signals closely matched, with shock arrival times, pressure rise times, and decay characteristics in agreement within the sampling resolution of the instruments.

D. Pre-Strain Capability Demonstration

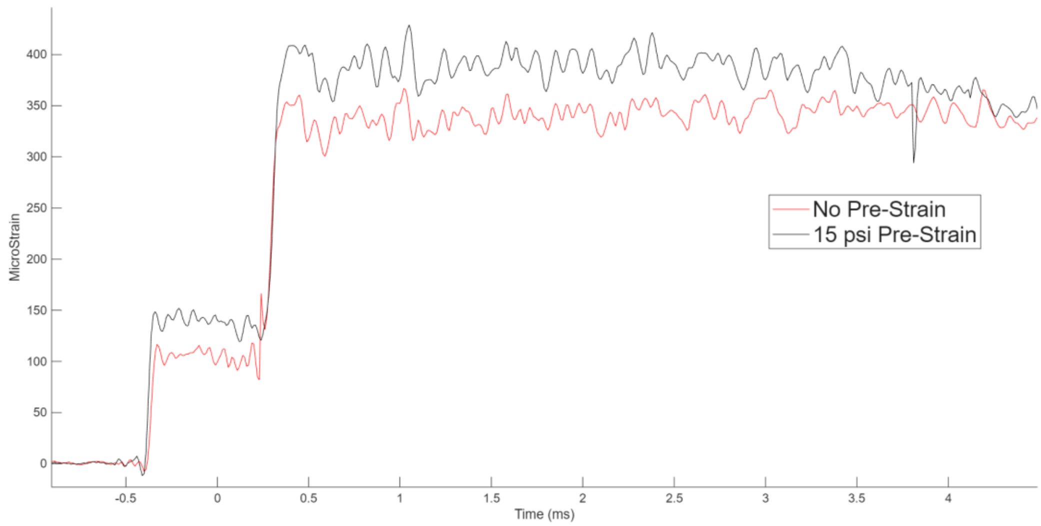

Fig. 9 Pre-strain effect on dynamic response showing hoop and axial strain comparisons between zero pre-strain and 15 psi pre-strain condition in carbon fiber

Under pre-strain conditions, the peak total hoop strain reached approximately 400 micro strain, compared to 300 micro strain without pre-strain. However, interpretation of this result is complicated by the fact that pre-pressurization of the driven section alters the strength of the shockwave.

This change in shock strength makes it difficult to isolate the true effect of pre-strain on structural behavior from the effect of increased dynamic loading magnitude. The observed increase in peak strain could result from: (1) initial pre-strain simply adding to the dynamic response, (2) the higher-pressure rise producing proportionally higher dynamic strain, or (3) some combination of both effects. Separating these contributions would require systematic testing at matched shock strengths with and without pre-strain, requiring a varied selection of diaphragm materials and burst pressures, which was beyond the scope of the present facility demonstration.

IV. Conclusions and Future Work

A shock-tube-based experimental facility has been developed and demonstrated for measuring time-resolved axial and hoop strain in cylindrical airframe structures subjected to controlled dynamic internal pressure loading. The facility successfully integrates interchangeable composite and metallic test sections into a conventional shock tube, transforming a gas-dynamics apparatus into a structural testing platform where the test article becomes an active pressure vessel subjected to two-stage loading from incident and reflected shocks.

Testing revealed that an isotropic specimen exhibited strong Poisson coupling between hoop and axial strain with synchronized 2:1 magnitude ratio and shared frequency content throughout the loading event. Whereas, a carbon fiber composite specimen demonstrated weak coupling with largely independent hoop and axial response, with minimal axial strain during hoop loading, and separated frequency content arising from orthotropic material properties and dissipation mechanisms. The end wall reflection and associated boundary constraint proved essential for revealing these coupling differences, as the incident shock alone produces primarily hoop-dominated response in both materials.

The demonstrated facility provides repeatable two-stage pressure loading, direct material comparison under identical conditions, high-bandwidth strain measurement in both directions, and interchangeable test section design, along with providing a test platform for evaluating FBG sensors for flight integration. Future work will include parametric layup studies to quantify fiber orientation effects on strain coupling, investigation of pre-strain effects with matched shock conditions, and systematic numerical model validation. This facility enables high strain-rate structural testing of composite airframe components and establishes a controlled platform for aerospace structural health monitoring and dynamic characterization studies.

V. Acknowledgments

The authors would like to thank the FOSS team at NASA Armstrong for in-house training with the FBG Interrogation system and FOSS hardware. The research conducted at the Vanderbilt Aerospace Design Laboratory was supported by the Mark Dalton Funds for Experiential Learning in Aerospace Engineering.

References

[1] Tzeng, J. T. "Dynamic Response and Fracture of Composite Cylinders." *Composites Science and Technology* 58, no. 9 (1998): 1443–51. https://doi.org/10.1016/S0266-3538(98)00021-9.

[2] Tzeng JT, Hopkins DA. Dynamic Response of Composite Cylinders Subjected to a Moving Internal Pressure. *Journal of Reinforced Plastics and Composites*. 1996;15(11):1088-1105. doi:10.1177/073168449601501102

[3] Khawaja, H. A., Bertelsen, T. A., Andreassen, R., Moatamedi, M., Study of CRFP Shell Structures under Dynamic Loading in Shock Tube Setup, *Journal of Structures*, 2014, 487809, 6 pages, 2014. https://doi.org/10.1155/2014/487809

[4] Chung, Deborah DL. *Carbon fiber composites*. Butterworth-Heinemann, 1994, pp. 85-110

[5] Jones, Robert M. *Mechanics of composite materials*. CRC press, 2018.

[6] Krishnamurthy, K. S.; Mahajan, P.; Mittal, R. K. Impact Response and Damage in Laminated Composite Cylindrical Shells. *Composite Structures* 2003, *59* (1), 15–36. https://doi.org/10.1016/S0263-8223(02)00238-6.

[7] Bourne, N. K.; Parry, S.; Townsend, D.; Withers, P. J.; Soutis, C.; Frias, C. Dynamic Damage in Carbon-Fibre Composites. *Philosophical Transactions of the Royal Society A: Mathematical, Physical and Engineering Sciences* 2016, *374* (2071), 20160018. https://doi.org/10.1098/rsta.2016.0018.

[8] Sun, J.; Huang, L.; Dai, Y. Dynamic Response and Damage Accumulation of Laminated Composites under Repeated Low-Velocity Impacts. *Materials (Basel)* 2023, *16* (2), 778. https://doi.org/10.3390/ma16020778.

[9] Wang, C.; Chen, Z.; Silberschmidt, V. V.; Roy, A. Damage Accumulation in Braided Textiles-Reinforced Composites under Repeated Impacts: Experimental and Numerical Studies. *Composite Structures* 2018, *204*, 256–267. https://doi.org/10.1016/j.compstruct.2018.07.084.

[10] Anderson, M., Puranik, B., Oakley, J. *et al.* Shock tube investigation of hydrodynamic issues related to inertial confinement fusion. *Shock Waves* 10, 377–387 (2000). https://doi.org/10.1007/s001930000067

[11] Panopoulou, A., Loutas, T., Roulias, D., Fransen, S., and Kostopoulos, V., "Dynamic fiber Bragg gratings based health monitoring system of composite aerospace structures," *Acta Astronautica*, Vol. 69, 2011. https://doi.org/10.1016/j.actaastro.2011.05.027.

[12] Mrad, N., "Potential of bragg grating sensors for aircraft health monitoring," *Transactions of the Canadian Society for Mechanical Engineering*, Vol. 31, 2007. https://doi.org/10.1139/tcsme-2007-0001.

[13] Cusano, A., Cutolo, A., Nasser, J., Giordano, M., and Calabrò, A., "Dynamic strain measurements by fibre Bragg grating sensor," 2004. https://doi.org/10.1016/j.sna.2003.10.031.

[14] James, S.W., Tatam, R. P., Fuller, S. R., and Crompton, C., "Monitoring transient strains on a gun barrel using fibre Bragg-grating sensors," *Measurement Science and Technology*, Vol. 10, 1999. https://doi.org/10.1088/0957-0233/10/2/002.

[15] "X-T Diagram Tools", University of Wisconsin-Madison, Department of Engineering Physics, https://silver.neep.wisc.edu/~shock/tools/xt.html